Journal of Engineering and Applied Science

RESEARCH Open Access

Influence of steel plates on the compressive strength and pore structure of concrete

Jing Wang and Xin Zhang*

*Correspondence: zhxingzy@163.com

School of Civil Engineering, Chongqing Industry Polytechnic College, No.1000 Taoyuan Avenue, Airport, Yubei District, Chongqing 401120, China

Abstract

To accurately predict the strength of concrete in a combined structure, this paper analyzed the effect of steel plates on the pore structure and strength of concrete. Two concrete strengths and eight steel plate thicknesses were used for the experimental specimens, and their pore structures and strengths were tested at 3, 7, and 28 days. It was found that the pore structure of concrete increased with the increase in steel plate thickness. Additionally, the strength of concrete decreased with the increase in steel plate thickness. Besides, an equation was proposed to predict the strength of concrete in specimens with steel plates in this research.

Keywords: Steel plates, Concrete, Compressive strength, Pore structure

Introduction

Concrete's cement-based material strength closely connects with the internal pore structure [1–5]. Many researchers have studied the association between the compressive strength and pore structure of concrete. For instance, Li established a method of influencing coefficients through pore diameter to predict the association between the compressive strength and pore structure of concrete [6]. Huang et al. used the relative specific surface area of concrete pores to predict the strength of concrete [7]. Lian et al. discussed the association between the compressive strength and pore structure of porous concrete [8]. Gao et al. studied the association between the compressive strength and pore structure of concrete specimens with pore defects [9]. Despite the different contents of these studies, researchers recognize the conclusion that the increased density of pore structure leads to an increase in the strength of concrete [6–12].

The pore structure of concrete will change when its deformation is constrained. According to research [13, 14], concrete specimens with expansion agents have denser pore structures when their expansive deformation is constrained. Due to the lack of relevant research, however, the change in the concrete pore structure remains unclear when the decrease of concrete volume is constrained.

When concrete is cast, cement will hydrate and consume the water inside the concrete, thus causing capillary stress on the pore wall inside the concrete. Capillary stress, combined with the drying effect and other factors, will decrease concrete volume, known as shrinkage [15]. With the continuous development of composite structure, steel sheet-concrete

composite structure has been applied in an increasing number of projects. Researchers have found that steel plates can inhibit the shrinkage of concrete and this inhibition effect produces restrained stress inside concrete in the opposite direction of shrinkage, thus reducing the decrease of concrete volume caused by shrinkage [16]. When reinforced with steel plates of different thicknesses, concrete specimens will see a decrease of 30 to 80% in shrinkage compared with plain concrete. According to past research on the association between the compressive strength and pore structure of concrete and the research results of the relationship between constraint and the concrete pore structure [15], it can be reasonably inferred that the reinforcement of steel plates will increase the concrete pore structure due to the constraint of steel plates and then decrease the compressive strength of concrete. However, this inference has not yet been proved.

Researchers have always been highly concerned about the strength of concrete and its influencing factors, especially for the composite structure. In structural design, selecting correct concrete strength parameters that accord with the actual situation is a vital link related to the structural safety and the normal function of the structure. If the inference presented in this study is confirmed, the concrete strength parameters used in the structural design will be higher than the practical values, which poses risks to the structure's safety. At the same time, in the construction process, the strength of concrete is an essential basis to judge whether concrete blinding and supporting scaffolds can be dismantled. Following Chinese codes [17], the strength of general concrete components shall reach 75% of design strength to remove support, while that of important concrete components shall reach 100% of design strength. In the past, consideration was not given to the influence of constraint on concrete strength. Therefore, the strength of plain concrete specimens determined whether the concrete strength met the requirements. The provisions of existing codes may increase the risk of engineering accidents if research shows that constraint increases the concrete pore structure and reduces the concrete strength.

As described earlier, the pore structure of concrete in a combined structure may be increased by the shrinkage of the concrete due to the restraint of the steel plates, which in turn may lead to a reduction in the strength of the concrete. However, seldom studies have been carried out to confirm this possibility. The actual strength of the concrete in a combined structure composed of steel plates and concrete is directly related to the safety of the structure and the construction process. Therefore, in this study, the influence of steel plates on the pore structure and compressive strength of concrete was discussed using tests. The mercury injection method tested the pore structure specimens with two grades of strength (C20, C50) and eight steel plate thicknesses at 3, 7, and 28 days. Meanwhile, all types of specimens were also tested for the cube compressive strength. The changes in the pore structure caused by steel plates and the resultant change rule of concrete strength were studied by comparing the compressive strength and pore structure of concrete with steel plates of different thicknesses.

Methods

This research aimed to analyze the effect of steel plates on the pore structure and compressive strength of concrete, and tests were conducted for 3, 7, and 28 days on pore structure specimens with C20 and C50 strength grades and eight steel plate thicknesses using the mercury injection method; also, all types of specimens were tested for cubic

Table 1 Mix proportions of concrete (kg/m^3)

Mix	Water/ binder ratio	Cement	Water	Fly ash	Sand	Coarse aggregate	Polycarboxylate superplasticizer
C20	0.50	290	175	60	825	950	9.1
C50	0.31	450	160	70	704	1056	11.2

Table 2 Chemical compositions of cementitious materials(%)

Composition (mass)	Cement	Fly ash
SiO_2	21.47	49.47
CaO	65.77	4.45
Al_2O_3	5.47	20.67
Fe_2O_3	4.28	14.32
MgO	1.44	1.17
SO_3	0.52	1.40

compressive strength. Furthermore, by comparing the compressive strength and pore structure of concrete with different thicknesses of steel plates, the changes in the pore structure caused by the steel plates and the resulting change in the strength of concrete were analyzed.

The concrete specimens in this study were cured in a standard curing chamber at a temperature of 20°C ± 2°C and a relative humidity of 65 ± 5%. The specimens in the standard curing room were placed on stands and were spaced 10 to 20 mm apart from each other, and the surfaces of the specimens were kept moist. When the specimens reached the test age, they were checked for size and shape after being removed from the conservation site. The dimensional tolerances met the specifications of the standard and were tested within 1 day. The characteristics of the materials used, the mixing ratios, and the specific procedure of the tests are described in Test section of this study. Results and discussion section contains a discussion and analysis of the experimental results and the four main conclusions presented in Conclusions section. This research has no human participants, data, tissue, or animal studies.

Test

Materials and mix proportions

Table 1 displays the mixed proportions of the two kinds of concrete. Table 2 shows the chemical compositions of fly ash and cement as cementitious materials. The specific surfaces of cement and fly ash were 3471 cm^2/g and 4680 cm^2/g, and density is 3.10 g/cm^3 and 2.22 g/cm^3, respectively. Coarse aggregate is crushed limestone with a maximum particle size of 20 mm, while fine aggregate is quartz sand with a fineness modulus of 3.0.

Specimens for testing the strength of concrete

In order to investigate whether the strength of concrete changes in a combined structure because the steel plates restrain the shrinkage of concrete. Thus, in this study, we tested the strength of concrete under different shrinkage conditions. The shrinkage

strain of the concrete is the ratio of the shrinkage deformation of the concrete to the specimen size (length, width, or height) along the shrinkage direction, which makes the shrinkage strain of the concrete independent of the specimen size. Thus, a small-size specimen is often used when studying the problems caused by concrete shrinkage [15, 16]. In this study, the specimen size used to conduct the test was 200 mm×200 mm×500 mm.

The moulding of specimens was completed with the detachable Teflon mould. Before the casting of specimens, two layers of Teflon film with a thickness of 1mm were laid at the mould's bottom. The mould was removed from all sides when the concrete was initially set. The above method ensured that steel plates only constrained concrete.

This study contained 18 types of specimens, including two different kinds of concrete strength (C20 and C50) and eight steel plate thicknesses (4, 6, 10, 12, 16, 20, 25, and 30 mm). To measure the constraint effect of steel plates, the ratio of the cross-sectional area *As* of steel plates to that *Ac* of concrete was defined as the constraint ratio:

$$\lambda = A_s/A_c \tag{1}$$

Table 3 shows the details of the specimens. Steel plates of different thicknesses were laid at the bottom of concrete specimens to meet the requirements of the test design (Fig. 1), according to Table 4. When pouring the specimen, the plate was first placed at the bottom of the Teflon mould, followed by pouring the concrete. Each specimen was thoroughly vibrated according to the requirements of Chinese specifications GB50081 [18]. When the concrete was initially set, the detachable Teflon mould was removed, so the steel plate only constrained the concrete.

Table 3 Detail of specimens

No.	Strength grades	The thickness of steel plates (mm)	Constraint ratio (%)
C20-R0	C20	0	0.0
C20-R1		4	2.0
C20-R2		6	3.0
C20-R3		10	5.0
C20-R4		12	6.0
C20-R5		16	8.0
C20-R6		20	10.0
C20-R7		25	12.5
C20-R8		30	15.0
C50-R0	C50	0	0.0
C50-R1		4	2.0
C50-R2		6	3.0
C50-R3		10	5.0
C50-R4		12	6.0
C50-R5		16	8.0
C50-R6		20	10.0
C50-R7		25	12.5
C50-R8		30	15.0

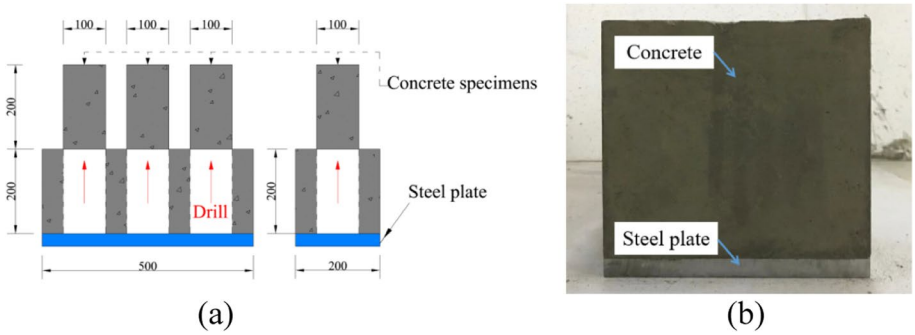

Fig. 1 Setup for the testing of physical properties and pore structure (mm): **a** specimen; **b** specimen after pouring. Note: The white part of (**a**) means the cavity left in the rectangular specimen after the cylindrical specimen was removed

Table 4 Properties of the steal plate

	Material	Elastic modulus ($\times 10^4$ MPa)	Yield strength (MPa)	Ultimate strength (MPa)
Steel plate	Q345A	21.1	395.0	550.0

The concrete compressive strength at different ages was tested by preparing three specimens of each type. The stable environment (20 ± 2°C, 65 ± 5% relative humidity) was used to cure and test all specimens.

At test ages (3, 7, and 28 days), three cylindrical specimens (height/diameter=2) with a diameter of 100 mm and a height of 200 mm were respectively drilled by a drill from the samples of each type of component according to the relevant requirements of JGJ/T384 [19] to test the concrete compressive strength, and the result was derived from the mean value of the three samples (Fig. 1). The test method of concrete strength was adopted according to the Chinese national standard GB/T50081 [18].

Specimens used for testing the porosity of concrete

The porosity of plain concrete specimens (C20-R0 and C50-R0) and concrete specimens reinforced with steel plates with a thickness of 6, 12, and 25 mm (C20-R2, C20-R4, C20-R7, and C50-R2, C50-R4, C50-R7) was tested. The specimens used for testing the porosity of concrete are the same as those used for testing the strength of concrete. At test ages, the remaining specimens were sampled for testing the porosity of concrete after cylinders used for testing the strength of concrete were drilled from the specimens. First of all, the removed concrete was squashed, and concrete particles of 2.5 to 5 mm were selected with a sieve. Second, acetone stopped the concrete from hydrating, and the sample was dried with a vacuum dryer. Lastly, the pore structure was tested with an AutoPore IV9510 automatic mercury porosimeter. Each test result comes from the average of the three test samples on the same specimen.

Results and discussion

Pore structure

Table 5 shows the pore structure parameters of plain concrete specimens (C20-R0 and C50-R0) and specimens with 6, 12, and 25 mm steel plates (C20-R2, C20-R4, C20-R7, and C50-R2, C50-R4, C50-R7) at 3, 7, and 28 days, including median and average pore diameters, the critical diameter of the capillary, porosity, and pore distribution. Each test result comes from the average of the three test samples on the same specimen. In terms of the test results, for the same specimen, no significant differences between the test results were found at the same age except for the very individual results.

It can be found from the table that the concrete pore structure gradually decreased as the concrete age increased when the mix proportion of concrete was the same as

Table 5 Pore characteristic parameters of specimens

	Average pore diameter (nm)	Median pore diameter (nm)	Critical diameter of capillary (nm)	Porosity (%)	Pore distribution (%)			
					<10 nm	10–50 nm	50–100 nm	>100 nm
C20-R0								
3	33.89	80.54	76.65	24.75	15.33	8.91	39.19	36.66
7	20.37	75.21	62.61	22.77	6.64	23.14	35.22	35.00
28	18.74	39.66	47.68	19.94	13.29	31.99	27.19	27.54
C20-R2								
3	36.51	85.64	81.42	25.79	21.64	11.69	35.09	31.59
7	22.54	70.53	69.92	24.74	19.11	31.14	28.95	20.81
28	20.46	40.36	49.61	22.15	21.67	37.33	19.19	21.81
C20-R4								
3	39.95	92.66	92.47	28.66	10.99	8.28	45.97	34.76
7	26.14	88.50	60.33	26.54	12.63	29.70	24.97	32.70
28	23.68	52.76	66.32	25.61	20.74	32.45	23.54	23.26
C20-R7								
3	46.03	106.53	100.19	31.31	13.62	13.96	36.96	35.46
7	35.85	91.60	90.47	28.71	22.41	18.38	32.70	26.51
28	27.61	69.56	67.17	26.88	25.41	27.29	25.39	21.91
C50-R0								
3	28.17	76.53	73.65	20.97	16.09	45.23	14.93	23.74
7	23.85	45.26	53.62	16.24	17.71	50.23	15.24	17.05
28	20.52	30.63	22.52	13.83	21.89	64.95	6.10	7.05
C50-R2								
3	30.83	80.22	80.89	26.04	12.58	48.62	22.34	16.56
7	28.33	54.40	58.65	18.40	13.44	62.25	15.14	9.17
28	22.40	38.58	35.44	16.86	22.51	64.66	10.70	2.13
C50-R4								
3	35.59	86.26	89.47	28.32	10.55	52.02	20.62	16.81
7	30.26	55.19	66.79	22.20	11.67	57.69	14.65	16.00
28	26.32	42.95	42.31	18.50	22.69	61.93	6.05	9.32
C50-R7								
3	40.66	95.07	97.11	30.40	19.29	38.53	24.56	17.63
7	35.23	67.61	81.26	25.33	7.56	53.16	19.99	19.30
28	31.24	50.42	56.26	21.79	11.26	64.35	16.87	7.53

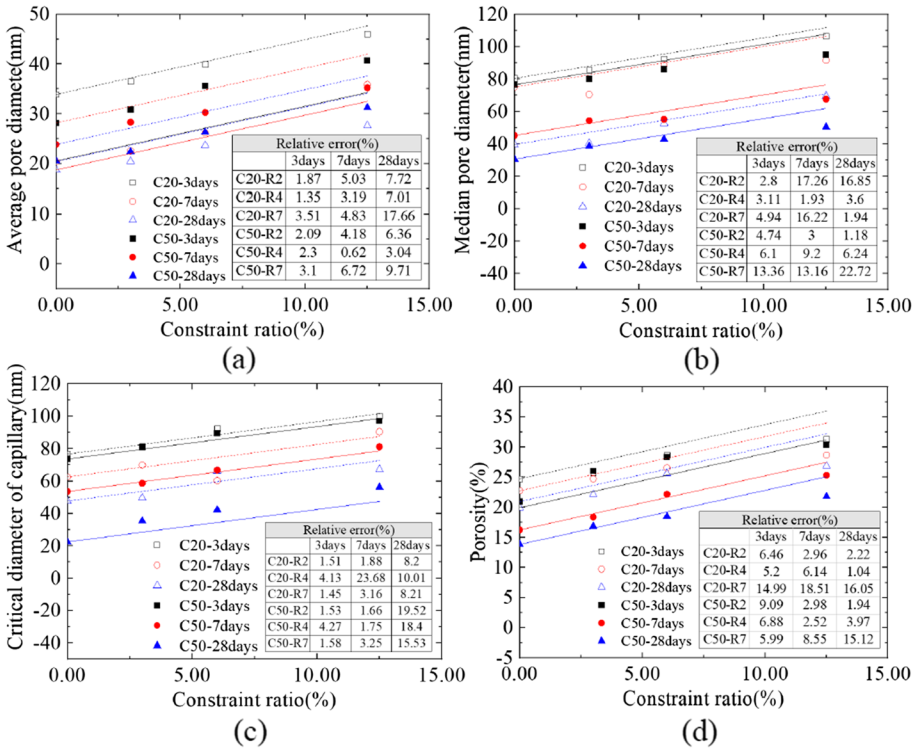

Fig. 2 Relationships between pore structure parameters and reinforcement ratio: **a** average pore diameter, **b** median pore diameter, **c** critical diameter of capillary, and **d** porosity

the thickness of steel plates. Take plain concrete specimen C20-R0 as an example. It is average, and median pore diameters, the critical diameter of capillary and porosity was 33.89 nm, 80.54 nm, 76.65 nm, and 24.75% at 3 days, but dropped to 18.74 nm, 39.66 nm, 47.68 nm, and 19.94% at 28 days. Meanwhile, pores less than 50nm accounted for 45.28% of all pores at 28 ages, which is greater than 24.24% at 3 days. This phenomenon was mainly due to the fact that the hydration products of cement filled in pores, and the capillary wall produced capillary stress after water consumption in concrete [20–23].

By comparing the specimens with the same mix proportion but different steel plate thicknesses, it can be found that the pore structure of concrete increases as the steel plate thickness increases at the same age. For example, the median and average pore diameters, the critical diameter of capillary and porosity of C20-R7 specimen reinforced with 25-mm steel plate at 28 days were 27.61 nm, 69.56 nm, 67.17 nm, and 26.88%, respectively, which are significantly greater than those of C20-0 specimen without steel plates, C20-R2 specimen with 6-mm steel plates and C20-R4 specimen with 12-mm steel plates. This phenomenon can also be observed in each C50 specimen with different mix proportions.

The relationship between the pore structure of concrete and the constraint ratio of steel plates is presented in Fig. 2 to more clearly show the changes in the pore structure caused by the constraint effect of steel plates. This indicates that the concrete pore structure increases as the constraint coefficient of steel plates on concrete increases. The following formula can represent the relationship:

Table 6 Values of *m* for different pore parameters

	Average pore diameter (nm)	Median pore diameter (nm)	Critical diameter of capillary (nm)	Porosity
m	110	250	200	90

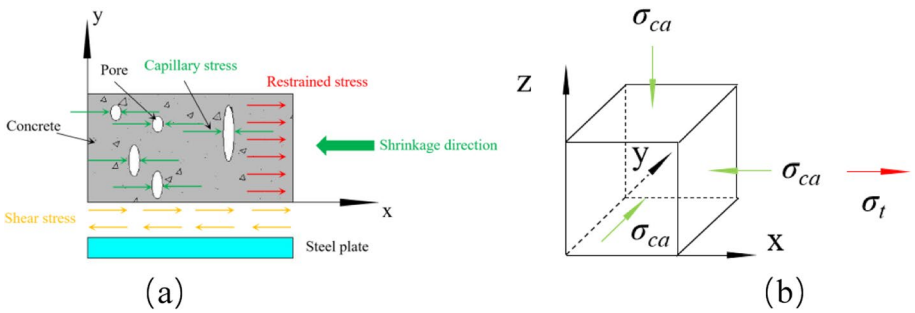

Fig. 3 Changes in the concrete pore structure: **a** Concrete shrinkage restrained by steel plate. **b** Concrete element

$$K_\lambda = k_0 + m_\lambda \tag{2}$$

where K_λ is the pore structure parameter of specimens reinforced with steel plates; k_0 represents the pore structure parameter of plain concrete; m refers to the change amount of pore structure when the unit constraint ratio increases.

In this study, k_0 is the pore structure parameter of plain concrete specimens (C20-R0 and C50-R0) obtained according to this test. Table 6 shows the parameter m calculated by the experimental data regression. Figure 2 shows the relative error between the measured value and the pore structure parameter of concrete. The table suggests that the measured values were consistent with the calculated ones.

Concrete is a porous material, where the consumption of water in concrete due to the hydration, drying effect, and other effects of cement will form capillary stress on the pores and microcracks of concrete. This capillary stress will reduce the concrete volume, often called shrinkage. The capillary stress effect and the filling of hydration products will lead to a decrease in the concrete pore structure [20–23]. When the shrinkage of concrete is constrained, shear stress will be generated at the interface between concrete and constraint (steel plates in this study) due to the non-deformation of the constraint itself. According to mechanical knowledge, this shear stress will generate normal stress in the opposite direction of shrinkage, which is so-called restrained stress.

Figure 3b shows a concrete component of a restrained specimen. According to the capillary tension theory, capillary stress is the critical driver of concrete shrinkage (σ_{ca}). In the specimen's length (x) direction, restrained stress and capillary stress apply to the concrete. This study suggests that since the inhibiting effect of the steel plate is mainly in the length (x) direction, only capillary stress applies to the concrete component in width (y) and height (z) directions. Using material mechanics, the concrete strain in length (x) direction ($\varepsilon_{c\text{-}x}$) is represented as follows:

$$\varepsilon_{c-x} = \frac{1}{E_c}\left[\sigma_x - \mu\left(\sigma_y + \sigma_z\right)\right] = \frac{1}{E_c}[(\sigma_{ca} - \sigma_t) - \mu(\sigma_{ca} + \sigma_{ca})] = \frac{\left(1 - 2_\mu\right)}{E_c}\sigma_{ca} - \frac{1}{E_c}\sigma_t \tag{3}$$

where σ_t is the restrained stress in the concrete. μ is the Poisson's ratio of the concrete. E_c is the elastic modulus of the concrete.

The shear stress at the concrete interface causes compressive stress in the steel plate (σ_{st}) and restrained tensile stress in the concrete. The formula can be derived according to the requirement of the force balance as follows:

$$A_c\sigma_t = A_s\sigma_{st} \tag{4}$$

As a result, the restrained stress in the concrete can be indicated as follows:

$$\sigma_t = \frac{A_s}{A_c}\sigma_{st} = \lambda\sigma_{st} \tag{5}$$

Only the compressive stress applies to the steel plate. In this way, the deformation strain of the steel plate ($\varepsilon_{st\text{-}x}$) in the x direction can be indicated as follows:

$$\sigma_t = \frac{A_s}{A_c}\sigma_{st} = \lambda\sigma_{st} \tag{6}$$

where E_{st} is the elastic modulus of the steel plate.

The concrete and steel plates have the same shrinkage strain in the restrained specimens. Thus,

$$\varepsilon_{c-x} = \varepsilon_{st-x} \tag{7}$$

Taking formulas (5), (6), and (7) into formula (2), the restrained stress in the concrete with the steel plate can be calculated as follows:

$$\sigma_t = \frac{(1 - 2\mu)}{1 + \frac{E_c}{\lambda E_{st}}}\sigma_{ca} \tag{8}$$

As shown in formula (8), the restrained stress in the opposite direction of capillary stress increases as the constraint ratio (i.e., the thickness of the steel plate) increases, thus lowering the reduction degree of the pore structure due to capillary stress. Therefore, the experimental results show that the pore structure of the concrete reinforced with the steel plate increases as the constraint ratio increases.

Compressive strength of concrete

The compressive strength of concrete specimens with different mix proportions under different constraint conditions is shown in Table 7, demonstrating that the concrete strength gradually increases with age when the mix proportion of concrete is the same as the steel plate thickness. The strength of concrete specimens at 3 and 7 days amounted to around 55 to 76% and 77 to 92% of that at 28 days, which is the same as the increased law of concrete strength observed in the past.

The strength of concrete changed dramatically after the reinforcement of steel plates. The concrete strength was inversely proportional to the thickness of the steel

Table 7 Test results of concrete strength (Mpa)

	3 days	7 days	28 days
C20-R0	14.6	18.5	23.5
C20-R1	14.0	17.7	21.5
C20-R2	13.2	15.5	19.5
C20-R3	12.3	14.5	18.6
C20-R4	12.2	13.5	16.0
C20-R5	8.9	12.5	16.1
C20-R6	8.6	11.9	15.4
C20-R7	8.9	11.6	14.6
C20-R8	7.0	10.1	12.5
C50-R0	38.4	45.0	52.0
C50-R1	35.6	43.5	51.5
C50-R2	29.6	42.7	47.6
C50-R3	27.8	40.8	44.3
C50-R4	25.4	38.5	42.4
C50-R5	23.5	36.5	41.5
C50-R6	21.1	30.1	37.6
C50-R7	19.8	28.9	32.5
C50-R8	17.5	26.5	30.5

plates. The thicker the steel plates were, the lower the strength of the concrete would be. Take C50 specimens as an example. The strength of the C50-R0 specimen at 28 days was 52.0 MPa. As the thickness of steel plates increases, the strength of C50-R1, C50-R2, C50-R3, C50-R4, C50-R5, C50-R6, C50-R7, and C50-R8 specimens dropped to 51.5 MPa, 47.6 MPa, 44.3 MPa, 42.4 MPa, 41.5 MPa, 37.6 MPa, 32.5 MPa, and 30.5 MPa, respectively.

This phenomenon was related to the changes in the concrete pore structure due to steel plates. The relationships between different parameters of pore structure and strength of concrete specimens under a constraint ratio of 3.0%, 6.0%, and 12.5% were shown in Fig. 4, which presents a negative correlation between the strength and pore structure of concrete. The smaller the concrete pore structure was, the higher the strength of the concrete would be. The restrained tensile stress generated by steel plates would weaken the reduction of capillary stress on the concrete pore structure. Thus, the pore structure of concrete reinforced with steel plates was larger, thereby leading to the lower strength of concrete. The thicker the steel plates were, the stronger the constraint effect would be. As a result, the strength of concrete decreased as steel plates increased.

Previously, researchers described the association between the compressive strength and pore structure of concrete using different models, such as linear, exponential, and polynomial relationships. In this work, the strength of the concrete also showed an excellent linear relationship with porosity and other parameters and increased with the decrease of porosity. However, it is worth noting that the strength of concrete with different mix proportions and the same pore structure parameters was significantly different, which is the same as the phenomenon observed by researchers before [24, 25]. For example, the porosity and compressive strength of the C20-R2 specimen at 3 days were 25.79% and 13.2MPa, but the strength of the C50-R2 specimen with a similar porosity (26.04%) reached up to 29.6 MPa.

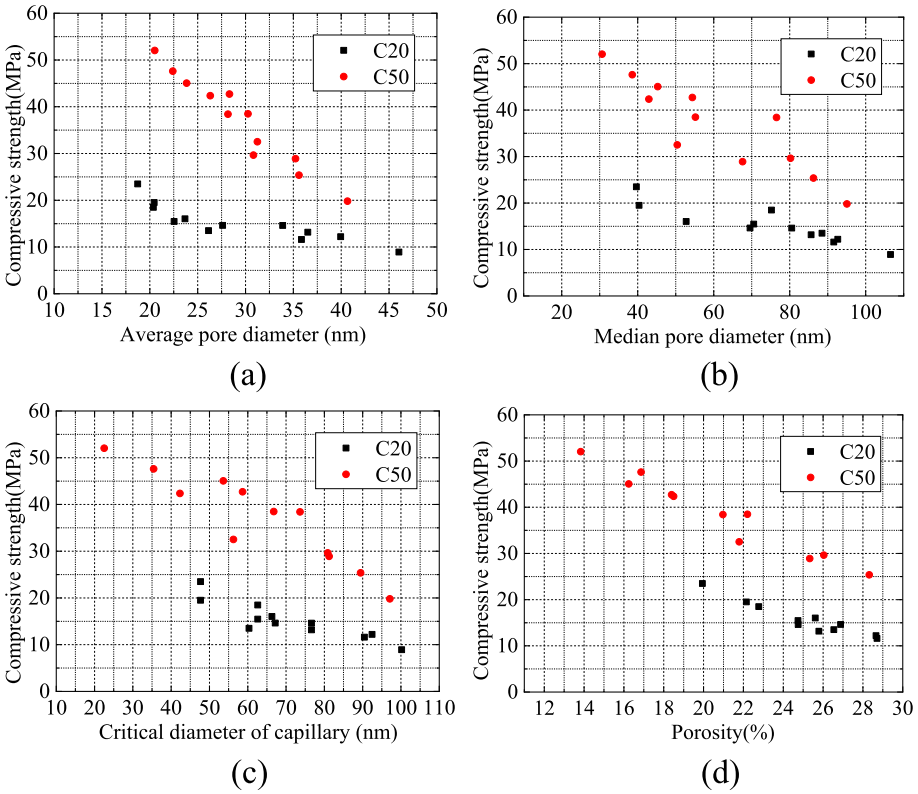

Fig. 4 Relationships between compressive strength and pore structure parameters: **a** average pore diameter, **b** median pore diameter, **c** critical diameter of capillary, and **d** porosity

This phenomenon may be related to the pore distribution of concrete pores. The pore distribution of C20 and C50 concrete specimens at all ages is illustrated in Fig. 5 and shows differences in law. The pore diameter of C20 concrete specimens is mainly distributed between 50 and 100nm, and the pore structure of C50 concrete specimens is principally composed of pores less than 50nm. Past research has suggested that the pore structure parameters (like median pore diameter and porosity) of concrete reflect all the pores of the concrete, and the difference in pore distribution may produce the same or different pore structure parameters [24, 25]. The smaller the pores constituting the concrete pore structure, the higher the concrete strength. Thus, it was observed that the strength of C50 concrete was higher than that of C20 concrete under the condition of similar pore structure parameters.

Relationship between the constraint ratio and compressive strength of concrete

According to previous research content, the constraint effect of steel plates on concrete would weaken the reduction of capillary stress on the pore structure and thus reduce the strength of concrete. The thicker the steel plates were, the stronger the constraint effect would be and the greater the loss of concrete strength would be. Therefore, it is necessary to consider the loss of strength caused by constraint in the case of designing and dismantling scaffolds in practical engineering, which, however, finds it difficult to determine the strength of concrete by testing pore structure, but easy to obtain the information on steel plates. In this case, a method of predicting the strength of concrete reinforced with steel plates using a constraint ratio was proposed in this study.

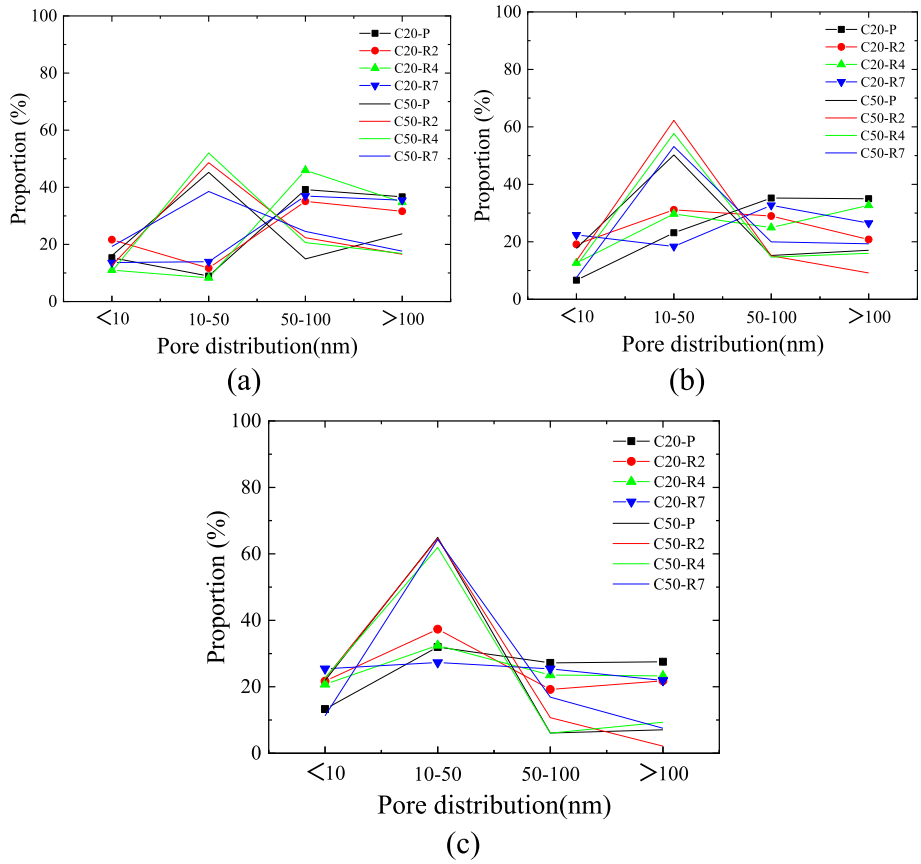

Fig. 5 Comparison between the pore distribution of C20 and C50 concrete specimens at different ages. **a** 3 days; **b** 7 days; **c** 28 days

$$f_{c\lambda} = f_{c0}\exp^{-n\lambda} \tag{9}$$

$f_{c\lambda}$ is the compressive strength when the constraint ratio is λ; f_{c0} represents the compressive strength when the steel plate thickness is 0. In this work, f_0 stands for the strength value of C20-R0 or C50-R0 concrete specimens, and n refers to the calculation parameter and n=4.6.

Figure 6 shows the strength of concrete reinforced with steel plates of different thicknesses predicted using Formula 3. At 3, 7, and 28 days, specimens reinforced with steel plates of different thicknesses have a mean prediction error of 7.03%, 1.65%, and 0.25%, and a maximum error of 13.87%, while C60 concrete has a mean prediction error of 10.41%, 10.54%, and 9.54%, and a maximum error of 14.93%, indicating that predicted values were in good agreement with actually measured ones.

Conclusions

In this study, the influence of steel plates on the pore structure and compressive strength was explored, and the structure and strength at different ages and with different steel plate thicknesses (constraint ratios) were tested. The following conclusions were drawn:

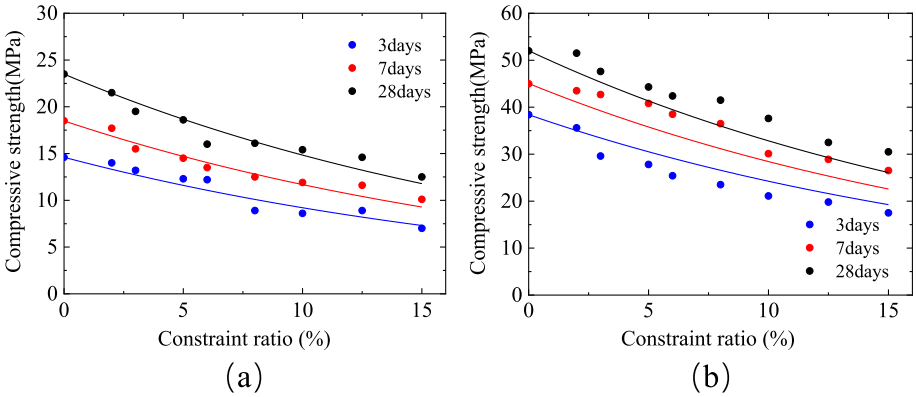

Fig. 6 Predicted results of Formula 3: **a** C20 concrete. **b** C50 concrete

(1) The concrete pore structure gradually decreased with age due to the effect of capillary stress and the filling of hydration products, and the proportion of pores less than 50 nm in all pores increased.
(2) Steel plates would have a constraint effect on concrete. The constraint effect would be more substantial with the increase of steel plate thickness and lead to an increase in the pore structure (median and average pore diameters, porosity, and critical diameter of capillary) of concrete. The changes in the pore structure constrained by steel plates can be predicted based on Linear Formula 2.
(3) The strength of concrete would decrease after the reinforcement of steel plates. The thicker the steel plates were, the lower the strength of the concrete would be, which was because steel plates weakened the reduction of capillary stress on the pore structure.
(4) The strength of concrete reinforced with steel plates was predicted by the formula using the strength of plain concrete and constraint ratio. As a result, the predicted values were consistent with actually measured ones.

Acknowledgements
The authors would like to acknowledge the Science and Technology Research Program of Chongqing Education Commission of China (Grant No. KJQN201803205) for financial support.

Authors' contributions
Jing Wang was a major contributor in writing the manuscript and conducted experimental analysis and comparison. Xin Zhang provided the data analysis, curation, and interpretation and corrected the grammar of the paper. The authors read and approved the final manuscript.

Funding
Sources of funding is from the Science and Technology Research Program of Chongqing Education Commission of China (Grant No. KJQN201803205).

Availability of data and materials
The datasets used and/or analyzed during the current study are available from the corresponding author on reasonable request.

Declarations

Competing interests
The authors declare that they have no competing interests.

Received: 26 September 2022 Accepted: 21 December 2022
Published online: 07 January 2023

References

1. Beaudoin JJ, Feldman RF, Tumidajski PJ (1994) Pore structure of hardened Portland cement pastes and its influence on properties. Adv Cem Based Mater 1:224–236
2. Rößler M, Odler I (1985) Investigations on the relationship between porosity, structure and strength of hydrated portland cement pastes I. Effect of porosity. Cement Concrete Res 15:320–330
3. Zhang G, Li Z, Zhang L, Shang Y, Wang H (2017) Experimental research on drying control condition with minimal effect on concrete strength. Constr Build Mater 135:194–202
4. Tufail M, Shahzade K, Gencturk B (2017) Effect of elevated temperature on mechanical properties of limestone, quartzite and granite concrete. Int J Concr Struct Mater 11:17–28
5. Szeląg M (2019) Properties of cracking patterns of multi-walled carbon nanotube-reinforced cement matrix. Materials 12:2942
6. Li D, Li Z, Lv C, Zhang G, Yin Y (2018) A predictive model of the effective tensile and compressive strengths of concrete considering porosity and pore size. Constr Build Mater 170:520–526
7. Huang YY, Ding W, Lu P (1984) The influence of pore-strucrure on the campressive strength of hardened cement paste. MRS Proc 42:123
8. Lian C, Zhuge Y, Beecham S (2011) The relationship between porosity and strength for porous concrete. Constr Build Mater 25:4294–4298
9. Gao H, Zhang X, Zhang Y (2015) Effect of the entrained air void on strength and interfacial transition zone of air-entrained mortar. J Wuhan Univ Technol-Mater Sci Ed 30(5):1020–1028
10. Balshin MY (1949) Relation of mechanical properties of powder metals and their porosity and the ultimate properties of porous metal-ceramic materials. Dokl Akad Nauk SSSR 67:831–834
11. Ryshkewitch E (1953) Compression Strength of porous sintered alumina and zirconia. J Am Ceram Soc 36:65–68
12. Hasselman DPH, Fulrath RM (1964) Effect of small fraction of spherical porosity on elastic moduli of glass. J Am Ceram Soc 47:52–53
13. Wang A, Sun D, Deng M, Chen X, Zhang F (2013) Influence of restraint on pore structures and air permeability of concrete containing MgO-type expansive agent. Asian J Chem 25:5532–5534
14. Zhang R, Wang Q, Ma L (2015) Relations between pore structure and creep characteristics of concrete under micro-expanding and lateral restraints. J Chin Ceram Soc 7:585–593
15. Huang L, Hua J, Kang M et al (2019) Capillary tension theory for predicting shrinkage of concrete restrained by reinforcement bar in early age. Conditions J Build Mater 210:63–70
16. Huang L et al (2019) Influence of steel plates and studs on shrinkage behavior and cracking potential of high-performance concrete. Materials 12(3):342
17. Ministry of Housing and Urban-Rural Development of the People's Republic of China (2011) Code for design of concrete structures (GB50666-2011). China Building Industry Press, Beijing
18. Ministry of Housing and Urban-Rural Development of the People's Republic of China (2019) Standard for test methods of concrete physical and mechanical properties (GB50081-2019). China Building Industry Press, Beijing
19. Ministry of Housing and Urban-Rural Development of the People's Republic of China (2016) China industry standards: technical specification for testing concrete strength with drilled core method (JGJ-T384-2016). China Building Industry Press, Beijing
20. Shen A (2000) Cement and cement concrete. China Communications Press, Beijing, pp 93–103
21. Li K, Luo M, Pang X, Zeng Q (2014) Pore structure of cement-based material under different curing conditions. J Build Mater 17:187–192
22. Flatt RJ, Scherer GW, Bullard JW (2011) Why alite stops hydrating below 80% relative humidity. Cement Concrete Res 41:987–992
23. Yang Q-B, Zhang S-Q (2004) Self-desiccation mechanism of high-performance concrete. J Zhejiang Univ-Sci A 5:1517–1523
24. Li Y, Li J (2014) Capillary tension theory for prediction of early autogenous shrinkage of self-consolidating concrete. Constr Build Mater 53:511–516
25. Gao H, Zhang X, Zhang Y (2013) Effect of Air Void structure on strength and interfacial transition zone of concrete. J Tongji Univ 42:0751–0756

Publisher's Note